

Hydrothermal–electrochemical CaTiO_3 coatings as precursor of a biomimetic calcium phosphate layer

J.P. Wiff^{a,c,*}, V.M. Fuenzalida^{a,c}, J.L. Arias^{b,c}, M.S. Fernandez^{b,c}

^a Departamento de Física, Fac. Cs. Físicas y Matemáticas, Universidad de Chile, Av. Blanco Encalada 2008, Santiago, Chile

^b Facultad de Ciencias Veterinarias, Universidad de Chile, Santa Rosa 11735, Santiago, Chile

^c Centro para la Investigación Interdisciplinaria Avanzada en Ciencia de los Materiales, Av. Blanco Encalada 2008, Santiago, Chile

Received 6 April 2006; accepted 11 June 2006

Available online 30 October 2006

Abstract

The hydrothermal–electrochemical method was used to coat Ti and Ti6Al4V with calcium titanate CaTiO_3 . The film exhibited a plate-like structure with several isolated pinholes around 100 nm in diameter. These coated samples were treated by a biomimetic procedure, immersing them in a simulated body fluid (SBF) solution for 5, 10 and 28 days. Characterization was performed by means of X-ray diffraction, X-ray photoelectron spectroscopy, scanning electron microscopy and energy dispersive spectroscopy. The CaTiO_3 -coated samples after the SBF treatment showed a significant increment in their calcium and phosphorous amounts as compared with SBF-treated samples with no previous CaTiO_3 coating; the latter exhibited only surface phosphate incorporation.

© 2006 Elsevier B.V. All rights reserved.

Keywords: Titanium; Coating; Calcium titanate; Biocompatibility; Hydrothermal; SBF

1. Introduction

Titanium and titanium alloys are extensively used as metallic implantable materials, due to their similar elastic modulus to human bone and their success in modern orthopaedic uses [1].

Several approaches have been implemented to enhance the biocompatibility of the titanium surface. One of them is coating the titanium implants with hydroxyapatite (HAp) $\text{Ca}_{10}(\text{PO}_4)_6(\text{OH})_2$. There are different methods to produce HAp coatings: sol–gel, physical vapour deposition (PVD) and plasma spray [2–4]. Generally speaking, these methods fail to coat substrates with a complex shape.

Another approach is the incorporation of calcium ions into the titanium substrate under the hypothesis that these ions may be able to enhance the osteointegration [5,6]. Ion implantation is a technique widely used for introducing calcium ions into the titanium surface because it leads to a faster bone growth [7]. However the

implantation requires complicated equipment or the use of high temperatures for crystallization. Other aqueous techniques have been used for introducing calcium ions on the titanium surfaces in order to simplify the ion implantation on titanium surfaces [8–11].

The hydrothermal process is a simple and powerful method for obtaining films ranging from hundreds of nanometers to a few micrometers grown on titanium substrates [9,12]. This method offers some distinct advantages, namely: a) comparatively low processing temperature, b) polycrystalline films grow without further annealing, c) good adherence, and d) it allows coating substrates of complex shape.

Calcium titanate (CT) has been suggested to provide a positive surface charge that interacts with the negatively charged phosphate ions in the fluid inducing the formation of a calcium phosphate layer [13]. Additionally CT has been reported as an intermediate in the biomimetic deposition of HAp [14]. Moreover, the CaTiO_3 layer acts as a calcium reservoir. Based on these ideas, we tried the fabrication of a CT coating having a thickness of hundreds of nanometers using the hydrothermal–electrochemical method (H–E). The objective was to introduce calcium (and magnesium) ions into the titanium and Ti6Al4V surface, in order to enhance the induction and natural self-

* Corresponding author. Present address: Nagaoka University of Technology, Department of Mechanical Engineering, Nagaoka Niigata 940-2188, Japan. Tel.: +81 8056 526 807; fax: +56 2 696 7359.

E-mail addresses: wiff@ishizaki.nagaokaut.ac.jp, jpwiff@yahoo.fr (J.P. Wiff).

fabrication of new tissue in the body, without prior deposition of synthetic HAp. In this work we report an *in-vitro* evaluation of CT coatings after treatment using a standard procedure with an SBF solution for 5, 10 and 28 days.

2. Experimental

2.1. Sample characterization

All samples, treated either only with H–E or immersed in the SBF solution, were characterized by XRD in a $\theta/2\theta$ Siemens D5000 diffractometer, with Cu K α radiation and a 0.02° scan step. XPS measurements were performed in a Physical Electronics 1257 system assisted with argon ion erosion at 4 keV. The argon erosion rate was estimated by placing a SiO₂-coated silicon wafer of known thickness in the system and measuring the time necessary to remove the SiO₂.

A scanning electron microscope (SEM), model JSM-JEOL 6301F, was used to observe the morphology. Electron dispersive spectroscopy (EDS), model JSM-6400+EDS Oxford Link Isis, at 10 kV was used to determine the local composition of the samples.

2.2. Substrate before the CaTiO₃ coating procedure

The substrates were either titanium plates (99.6%, Goodfellow TI000430/21) or biomedical titanium alloy plates (Ti6Al4V, Goodfellow TI010500/8) cut to $10 \times 10 \times 1$ mm, cleaned with acetone, ethanol and deionised water in an ultrasonic bath. Both substrates were characterized by XPS and XRD. Titanium, oxygen and carbon (adsorbed from the atmosphere) were detected on both types of substrates; aluminium and vanadium were also detected in the Ti6Al4V.

2.3. CaTiO₃ coating procedure

Saturated Ca(OH)₂ (J. T. Baker, Lot T08353, 97.8% with 0.3% of magnesium) aqueous solutions were prepared with hot deionised water, after boiling it to eliminate dissolved CO₂, and placed in a Teflon beaker. Excess NaOH was added as a mineraliser to the Ca(OH)₂ solution to adjust pH to around 13.5. The electrode and counterelectrode were both of the same material, either titanium or Ti6Al4V, separated by about 15 mm. The H–E process was performed in an autoclave at 200 °C, under a pressure of 2 MPa generated by the vapour, applying a DC current density of 25–30 mA/cm² between the electrodes during 30 min. These experimental conditions were selected after several tests and are close to those used to grow CT on a Ti–Al alloy [15]. A detailed description of the process and film properties is provided elsewhere [9]. No changes were detected in the CaTiO₃ films after ultrasonic cleaning.

2.4. Treatment in SBF solution

A SBF solution was prepared by dissolution of the chemicals in deionised water [16]. Control samples (i.e. titanium and Ti6Al4V without coating) as well as H–E-treated samples were immersed in the solution under a CO₂ flow of 0.1 l/min, at 37 °C. The SBF solution was changed every 48 h for 28 days. Samples were

extracted after 5, 10 and 28 days. After extraction the samples were washed with deionised water in an ultrasonic bath for 10 min and then dried in air at 50 °C.

3. Results and discussion

3.1. CaTiO₃ coating before the SBF treatment

Fig. 1 shows the XRD pattern of the H–E-treated samples. They exhibit reflections from orthorhombic calcium titanate (JCPDS 22-0153), superimposed on the reflections of the polycrystalline titanium substrate (JCPDS 44-1294). A minor phase of sodium titanate [14] was detected. No reflections of CaCO₃ were observed.

XPS analysis of the CT-coated titanium and CT-coated Ti6Al4V samples exhibited calcium, magnesium, oxygen, sodium and titanium on the surface of the film. Magnesium, present as an impurity in the starting Ca(OH)₂, was incorporated into the CT coating with a Ca:Mg ratio of $\sim 100:6$ [9]. The magnesium incorporation is of relevance in the present context because it has a determining role in the biomineralisation process [6]. Magnesium in solution is considered an inhibitor of HAp deposition, but at the surface it can enhance heterogeneous HAp nucleation [17].

The composition of the CT coating was the same on the titanium as well as on the Ti6Al4V substrates. The calcium XPS profile in Fig. 2a shows that its concentration in the CT coating decreases from the surface to the bulk. The thickness of the CT film estimated from the erosion rate was approximately 200–300 nm, which is in agreement with the thickness measured from a cross section using SEM [9]. After the H–E treatment, XPS did not detect either aluminium or vanadium on the surface in all these samples.

SEM analysis revealed a laterally heterogeneous microstructure, with a dominant plate-like growth attributed to CT and star-like shapes of CaCO₃ at some places, as shown in Fig. 3. The inset in Fig. 3 shows some pinholes of around 100 nm in diameter. The EDS analysis detected only oxygen and titanium at these pinholes.

3.2. CaTiO₃ coating after SBF treatment

After the treatment in SBF, the X-ray diffractogram did not show any change with respect to the X-ray pattern of Fig. 1, thus indicating that the crystallinity of the CT was not affected by the treatment. There were

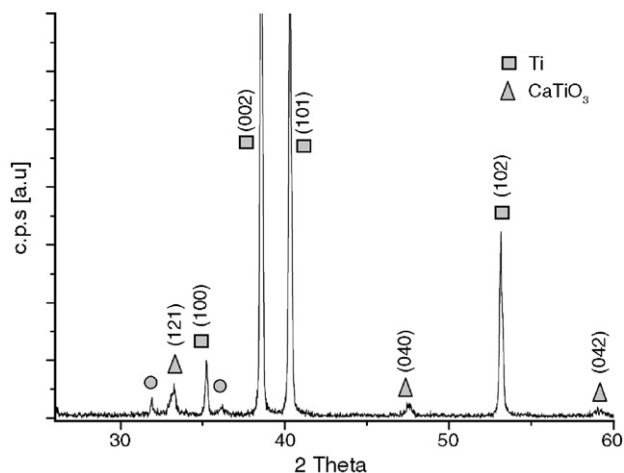


Fig. 1. XRD diffractogram of a CT-coated titanium sample. The squares, triangles and circles correspond to: titanium substrate, orthorhombic CaTiO₃ and sodium titanate respectively.

no new reflections of a calcium phosphate phase (whose existence was revealed by XPS and EDS measurements described later) because it was either amorphous, or nanocrystalline, or below the detection limit of XRD [8].

The XPS analysis at the surface revealed calcium, magnesium, oxygen, phosphorus and sodium, but not titanium. In every SBF-treated sample, i.e. CT-coated and non-coated sample (control sample), a phosphorus signal was detected. The binding energy of the P2p peak around 134 eV was in the range of the phosphates (not shown) [18]. This signal disappears after erosion with argon ions in the SBF-treated control samples, indicating that phosphorus enrichment occurs only at its surface.

Fig. 2b is an XPS depth profile of calcium and phosphorus performed on a CT-coated SBF-treated sample after immersion for 28 days in the SBF solution. The profiles show that the calcium concentration in the CT-coated SBF-treated samples was larger than that in the CT-coated sample (Fig. 2a) and was even larger than in the SBF-treated control samples (Fig. 2c). Fig. 2b shows that calcium is found to a depth beyond 700 nm after SBF treatment, much more than the original CT film (Fig. 2a), evidencing the deposition of a large amount of material. The depth distribution of phosphorus shows a behaviour similar to that

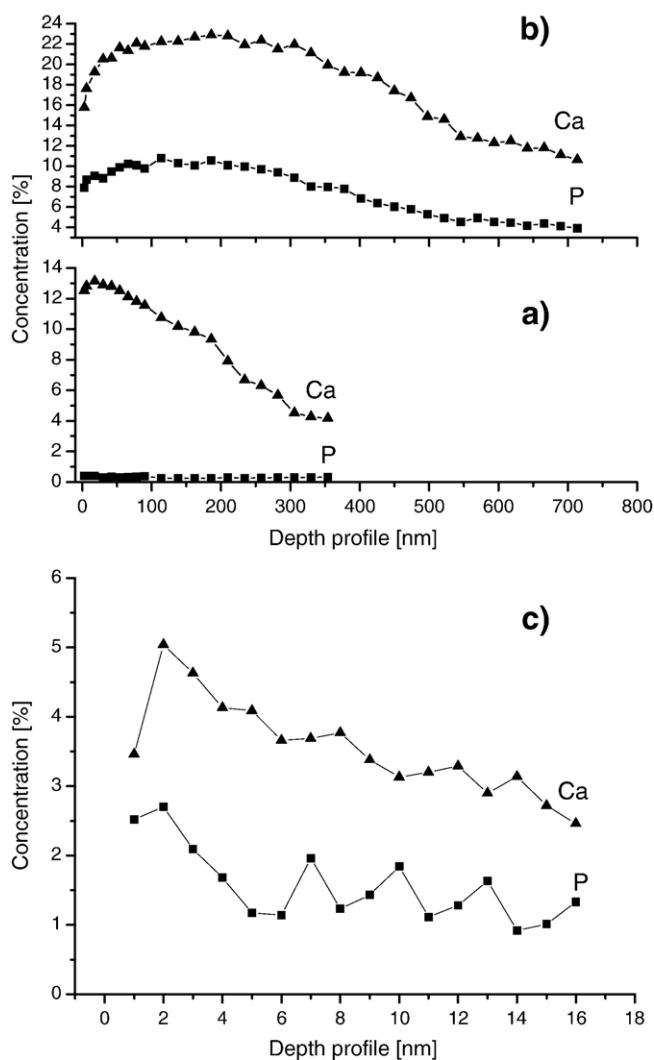


Fig. 2. Depth concentration profiles of calcium and phosphorus in different samples: a) CT-coated sample, b) CT-coated SBF-treated sample and c) non-coated SBF-treated sample.

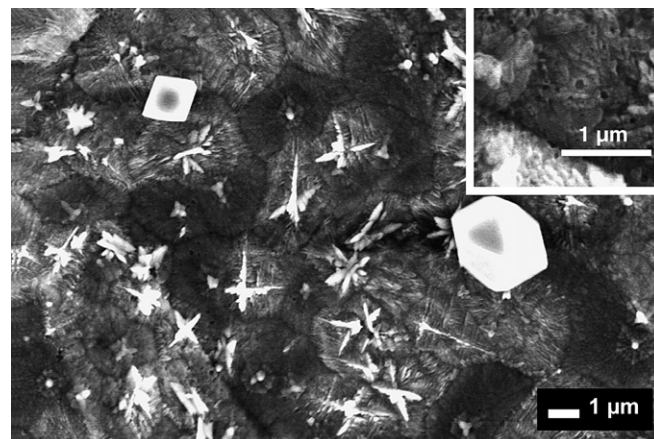


Fig. 3. SEM image obtained from the CT-coated titanium surface. The inset shows pinholes of approximately 100 nm in diameter.

of calcium. This indicates that a new layer containing calcium and phosphorus was deposited during the SBF treatment.

The morphology of a CT-coated sample SBF-treated under CO_2 flow for different periods is shown in Fig. 4. Micrograph a) shows the titanium SBF-treated control sample after immersion for 5 days, exhibiting no change with respect to the original titanium plate. The Ti6Al4V sample, not illustrated, shows the same behaviour. Fig. 4b) shows the microstructure of a CT-coated SBF-treated titanium sample (5 days), exhibiting new features (globule) on the surface. There are no significant changes after 10 days (not shown). Fig. 4c) shows the CT-coated SBF-treated sample immersed for 28 days, with regions populated with globules of around 1 μm in diameter. The pinholes indicated in Fig. 3 are still present (bottom left).

EDS detected calcium, magnesium, phosphorus, sodium, and titanium in every SBF-treated sample. Phosphorus had its highest concentration in the CT-coated SBF-treated sample within the globular structure (Fig. 5a), a lower concentration at the surface in the same kind of sample (Fig. 5b), and the lowest in the SBF-treated control samples (not shown). An important observation is that the composition at the pinholes is identical to the one observed before treatment in SBF, indicating that the CT coating is an essential step for the incorporation of the phosphate layer at the surface (Fig. 5c).

Fig. 5 revealed significant differences in phosphorus incorporation at different locations of the CT-coated SBF-treated samples. The composition found inside the pinholes was substantially different from the composition found at other places on the CT-coated samples, but is similar to TiO_2 , which corresponds to a sample without any CT coating at all. Phosphorus was not found inside the nano-pinholes, evidencing the influence of calcium at the beginning of the biomimetic process.

Notice that XPS signals carry information from a few nanometers below the surface, and EDS detects elements at a depth of several hundred nanometers. Therefore the high titanium signal detected by EDS originated in the substrate, below the biomimetic HAp layer. In Fig. 5a the relative titanium concentration is lower than in Fig. 5b and c because the new biomimetic layer reduces the effective beam penetration towards the titanium substrate.

The EDS measurements of Fig. 5a) and b) displayed a silicon peak on the CT-coated samples. Silicon was found only in the CT layer; no silicon was detected at the pinholes (non CT-coated zones, Fig. 5c). A detailed examination of the XPS spectra (not shown) revealed silicon at the hydrothermal CT layer, but not after the SBF treatment. This indicates that silicon was incorporated during the hydrothermal process.

After 28 days, the globular structure did not completely cover the CT-coated SBF-treated samples. This has several possible explanations.

The treatment time could be too short for this effect to be observed [19]. However shorter times have been reported for the coating of Ti6Al4V surfaces using SBF at a concentration five times higher [20]. These films, however, partially detached from surfaces with low roughness, indicated that roughness is of key importance in the mechanical attachment of the films. A quantitative roughness comparison is difficult, however, because the surface exposed to the solution in our case is chemically different. There are several surface treatments which promote the biomimetic deposition of HAp. We propose that one of the main advantages of hydrothermal CT coating as compared to surface treatments consists of providing a calcium reservoir that strongly adhered to the metallic substrate due to its diffuse interface. It is expected

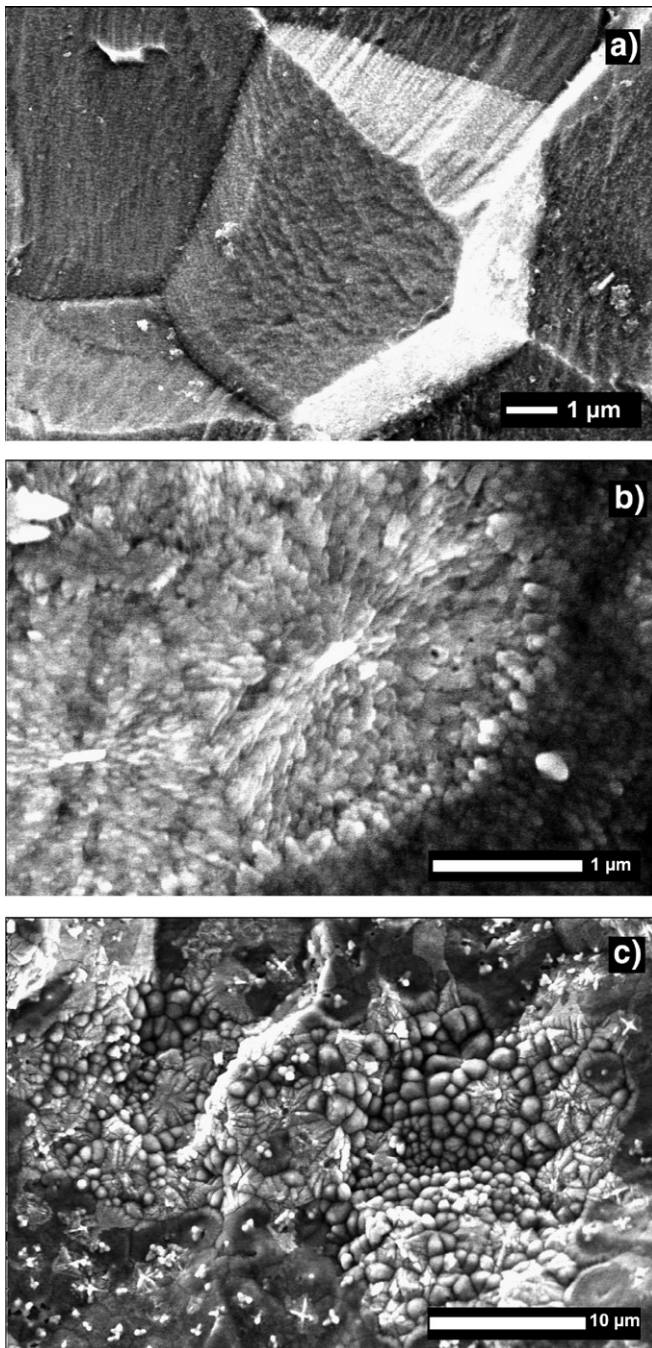


Fig. 4. a) SBF-treated control sample for 5 days. b) CT-coated SBF-treated sample for 5 days and c) 28 days.

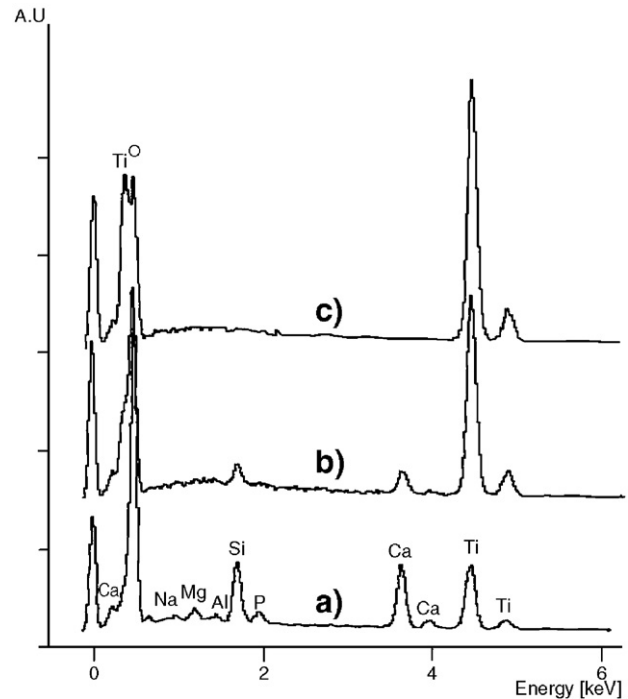


Fig. 5. EDS spectra from: a) the globular structure, showing a phosphorus signal, b) the CT-coated SBF-treated surface away from the globular structure, and c) nano-pinhole, where only titanium and oxygen were detected.

that the calcium reservoir will induce the growth of a new phosphate layer onto the CT, thereby providing an effective mechanism for generating a biomimetic layer.

Fig. 4c shows a heterogeneous coating of calcium phosphate (CT-coated SBF-treated samples). Jonásova et al. [21] treated titanium samples with HCl before NaOH activation and *in-vitro* calcium phosphate deposition from SBF. They showed that the acid etching is essential to dissolve the inhomogeneous TiO_2 – TiO_x layer that generally covers the titanium, leading to a homogeneous roughness as well as a thin TiO_2 –gel layer on the titanium samples, all of which favours the homogeneity of the coating. Our samples displayed a well formed calcium phosphate structure (Fig. 4c) even without any pre-treatment with acid solutions. It is expected that the HCl etching could increase the homogeneity of this coating.

4. Conclusions

A hydrothermal–electrochemical coating of $CaTiO_3$ on titanium or Ti6Al4V alloy favours the biomimetic deposition of hydroxyapatite (HAp). This appears from a near 500 nm HAp layer grown onto the $CaTiO_3$ -coated substrates. In this experiment pinholes in the $CaTiO_3$ layer were not coated with HAp. Test samples with no $CaTiO_3$ coating and pinholes exhibited only adsorbed phosphorous, without a phosphate layer. These results suggest that previous $CaTiO_3$ coating is an interesting method to enhance the biocompatibility of titanium and Ti6Al4V alloy.

Acknowledgments

This work was financed by the Chilean Government under grant FONDAF 11980002 and fellowships provided by

CONICYT. The surface analysis was possible thanks to Fundación Andes under grants c12510 and c12776. We thank also Prof. J. Bauer, Mona Mouallem and Mr. J. Le-Lanic for the SEM micrographs and Dr. M. Pilleux for valuable discussions.

References

- [1] M.C. Garcia-Alonso, L. Saldaña, G. Vallés, J.L. Gonzalez-Carrasco, J. Gonzalez-Cabrero, M.E. Martinez, E. Gil-Garay, L. Munuera, *Biomaterials* 24 (2003) 19.
- [2] S. Kačiulis, G. Mattogno, A. Napoli, E. Bemporad, F. Ferrari, A. Montenero, G. Gnappi, *J. Electron Spectrosc. Relat. Phenom.* 95 (1998) 61.
- [3] S. Kačiulis, G. Mattogno, L. Pandolfi, M. Cavalli, G. Gnappi, A. Montero, *Appl. Surf. Sci.* 151 (1999) 1.
- [4] L. Sun, C. Berndt, K. Khor, H. Cheang, K. Gross, *J. Biomed. Mater. Res.* 62 (2002) 228.
- [5] T. Horbett, B. Ratner, J. Schakenraad, F. Schoen, Some background concepts, in: B. Ratner, A. Hoffman, F. Schoen, J. Lemons (Eds.), *Biomaterials Science: an Introduction to Materials in Medicine*, Academic Press, San Diego, 1996.
- [6] M. Textor, C. Sittig, V. Frauchiger, S. Tosatti, D. Brunette, Properties and biological significance of natural oxide films on titanium and its alloys, in: D. Brunette, D. Tengvall, M. Textor, P. Thomsen (Eds.), *Titanium in Medicine: Materials Science, Surface Science, Engineering, Biological Responses and Medical Applications*, Springer-Verlag, Berlin, 2001.
- [7] T. Hanawa, Y. Kamiura, S. Yamamoto, T. Kohgo, A. Amemiya, H. Ukai, K. Murakami, K. Asaoka, *J. Biomed. Mater. Res.* 36 (1997) 131.
- [8] M. Manso, M. Langlet, J. Martínez-Duarte, *Mater. Sci. Eng., C, Biomim. Mater., Sens. Syst.* 23 (2003) 447.
- [9] J.P. Wiff, V.M. Fuenzalida, R.A. Zárate, J.L. Arias, M.S. Fernández, *J. Phys., Condens. Matter* 16 (2004) S1345.
- [10] X. Zhu, K. Kim, Y. Jeong, *Biomaterials* 22 (2001) 2199.
- [11] M.T. Pham, M.F. Maitz, W. Matz, H. Reuther, E. Richter, G. Steiner, *Thin Solid Films* 379 (2000) 50.
- [12] M. Yoshimura, S.-E. Yoo, H. Hayashi, N. Ishizawa, *Jpn. J. Appl. Phys.* 28 (1989) 2007.
- [13] H.M. Kim, H. Kaneko, M. Kawashita, T. Kokubo, T. Nakamura, *Key Eng. Mater.* 254-2 (2004) 741.
- [14] H. Takamada, H. Kim, T. Kokubo, T. Nakamura, *Sci. Technol. Adv. Mater.* 2 (2001) 389.
- [15] M. Yoshimura, W. Urushihara, M. Yashima, M. Kakihana, *Intermetallics* 3 (1995) 125.
- [16] T. Kokubo, H. Kushitani, S. Sakka, T. Kitsugi, T. Yamamuro, *J. Biomed. Mater. Res.* 24 (1990) 721.
- [17] F. Barrere, C.A. van Blitterswijk, K. de Groot, P. Layrolle, *Biomaterials* 23 (2002) 2211.
- [18] J. Moulder, W. Stickle, P. Sobol, K. Bomben, in: Jill Chastain (Ed.), *Handbook of X-ray Photoelectron Spectroscopy*, Physical Electronics (PHI), USA, 1992.
- [19] W. Song, Y. Jun, Y. Han, S. Hong, *Biomaterials* 25 (2004) 3341.
- [20] F. Barrere, M.M.E. Snel, C.A. van Blitterswijk, K. de Groot, P. Layrolle, *Biomaterials* 25 (2004) 2901.
- [21] L. Jonásöva, F. Müller, A. Helebrant, J. Strnad, P. Greil, *Biomaterials* 25 (2004) 1187.